



■ CHILDREN'S ORTHOPAEDICS

Dynamic deformation of the femoral head occurs on weightbearing in Legg-Calves-Perthes disease

A TRANSLATIONAL PILOT STUDY

**A. Aarvold,
R. Lohre,
H. Chhina,
K. Mulpuri,
A. Cooper**

University of British
Columbia, Vancouver,
British Columbia,
Canada

Aims

Though the pathogenesis of Legg-Calve-Perthes disease (LCPD) is unknown, repetitive microtrauma resulting in deformity has been postulated. The purpose of this study is to trial a novel upright MRI scanner, to determine whether any deformation occurs in femoral heads affected by LCPD with weightbearing.

Methods

Children affected by LCPD were recruited for analysis. Children received both standing weightbearing and supine scans in the MROpen upright MRI scanner, for coronal T1 GFE sequences, both hips in field of view. Parameters of femoral head height, width, and lateral extrusion of affected and unaffected hips were assessed by two independent raters, repeated at a one month interval. Inter- and intraclass correlation coefficients were determined. Standing and supine measurements were compared for each femoral head.

Results

Following rigorous protocol development in healthy age-matched volunteers, successful scanning was performed in 11 LCPD-affected hips in nine children, with seven unaffected hips therefore available for comparison. Five hips were in early stage (1 and 2) and six were in late stage (3 and 4). The mean age was 5.3 years. All hips in early-stage LCPD demonstrated dynamic deformity on weightbearing. Femoral head height decreased (mean 1.2 mm, 12.4% decrease), width increased (mean 2.5 mm, 7.2% increase), and lateral extrusion increased (median 2.5 mm, 23% increase) on standing weightbearing MRI compared to supine scans. Negligible deformation was observed in contra-lateral unaffected hips, with less deformation observed in late-stage hips. Inter- and intraclass reliability for all measured parameters was good to excellent.

Conclusion

This pilot study has described an effective novel research investigation for children with LCPD. Femoral heads in early-stage LCPD demonstrated dynamic deformity on weightbearing not previously seen, while unaffected hips did not. Expansion of this protocol will allow further translational study into the effects of loading hips with LCPD.

Cite this article: *Bone Joint Open* 2020;1-7:364–369.

Keywords: perthes disease, children, MRI

Correspondence should be sent to
Anthony Cooper; email:
externalfixators@cw.bc.ca

doi: 10.1302/2633-1462.17.BJO-
2020-0030.R1

Bone Joint Open 2020;1-7:364–
369.

Introduction

Legg-Calvé-Perthes disease (LCPD), though described over 100 years ago, remains elusive of aetiology, pathogenesis, or treatment consensus.^{1,2} However, the resulting deformity predisposes affected individuals to

early degenerative changes relative to their peers.³⁻⁵

While the stages of LCPD are well characterized, as described by the modified Waldenström classification,^{6,7} underlying patho-etiology of the deformity is not well understood. As such, wide variation exists in

treatment methods, duration, and timing. A consensus exists on treatment goals, namely to minimize ultimate deformity and postpone degenerative change, but how best to achieve this remains contentious.^{1,5,8} For example, degree of lateral femoral head pillar collapse,⁹ assessed on plain radiographs during the fragmentation stage, has been used for prognostication and treatment determination.¹⁰⁻¹³ Considering that once radiological evidence of femoral head deformity has occurred, and that radiological changes lag behind the disease process by three to four months, the window for treatment to prevent deformity occurring has been missed when using this algorithm.^{10,11,14}

Arthrography,¹⁵ bone scans, ultrasonography,¹⁶ and MRI are variably used, each with inherent advantages and disadvantages.¹⁵ MRI can detect LCPD in the early stages when plain radiographs remain normal, though availability and tolerance limit its utility.¹⁵ To date, prognostication of LCPD using MRI has not been proven, though contrast MRI scans have shown promise.¹⁷⁻²³ MRI features of necrotic extension, physeal involvement, metaphyseal changes, and lateral extrusion have been proposed as potential prognosticating values in early disease.^{20,22-24}

Repetitive forces applied through the femoral head while weightbearing may cause microfracture of the necrotic bone, deformation, collapse, and extrusion, which adversely affect prognosis.^{1,2,25,26} The effects of loading have been hypothesized, and improved outcomes demonstrated on porcine non-weightbearing studies.²⁶ Despite the proposed pathology of LCPD deformation occurring in a viscoelastic hip, any dynamic effects are not captured using current static imaging methods.

The MRI facility used in this study houses the world's only dedicated research upright open MRI scanner. This facility allows MRI to be performed in a functional weightbearing position. It has been utilized for imaging of patients with femoro-acetabular impingement (FAI)²⁷ and patellofemoral alignment²⁸ in functional weightbearing positions. However, until now, it has not been used for children in the age range of those with LCPD, nor have LCPD-affected hips had cross-sectional imaging while under functional loading conditions.

This study aims to explore the feasibility of using this novel weightbearing MRI in a younger patient age range and, specifically, whether it can be tolerated in children with LCPD. To successfully image an LCPD-affected femoral head under physiological loading would be entirely novel. Thus, this study aims to analyze all images for any detectable dynamic deformation on weightbearing compared to non-weightbearing images and unaffected femoral heads.

Methods

Institutional ethics review was completed prior to data collection (CW15 0002/H14 03407). Data was

prospectively collected on patients with LCPD presenting to the paediatric orthopaedic clinic at senior author's institution from April 2015 to February 2017. All children with LCPD were offered inclusion in the study. Children were excluded if the affected hip had undergone surgical intervention or the parent predicted inability to tolerate the standing MRI. Contralateral unaffected hips were used as controls. Consent to participate was obtained from the adult caregiver. All children received plain radiographs as part of their routine standard of care, from which the stage of disease was determined based on the modified Waldenstrom classification. Demographic data was collected (sex, age, laterality). MRI was acquired using the MROpen 0.5 Tesla upright scanner (Paramed Medical Systems, MROpen, Genova, Italy).

Protocol development

Imaging was performed on three healthy volunteers in the age range of those affected by LCPD to optimize patient positioning and image sequence acquisition. Weightbearing standing plus corresponding supine MRI was performed in the upright open MR scanner. Due to prediction that a child with an irritable hip will tolerate a supine scan more easily than a weightbearing scan, the upright images were acquired first, followed by the supine non-weightbearing images. A reproducible standardized weightbearing position was achieved by having both feet placed shoulder width apart on a foot map with the patellae pointing forward. Foam blocks and support bars were placed at the lumbar spine and chest to help subjects remain still during scanning, while not limiting the weight that was taken through the limbs (Figure 1). A receiver coil was placed around the pelvis and secured with straps and waist belt. The positioning protocol was mirrored when the child was supine, to obtain equivalent scans. Supine scans immediately followed the standing weightbearing scans. Each child wore headphones that were linked to a video monitor, with a wide choice of cartoons and films. The monitor was safely outside the MRI room but easily visible by the child from the standing position within the scanner. Healthy volunteers could tolerate longer in the scanner than those with irritable hips with LCPD. Thus scan duration for the children with LCPD was limited to 2.5 minutes.²⁸

Image acquisition

The MRI sequence protocol was developed with the assistance of the healthy volunteers. Satisfactory image acquisition was obtained with Coronal T1 GFE sequences, both hips in field of view (FoV), slice thickness 4 mm, slice gap 0.6 mm, TR 687 ms, TE 20 ms, NEX 1, FOV 200 mm, matrix 256 × 256. This protocol produced the readable images compared to other trialed sequences. Scan duration was limited to 2.5 minutes scans, with the child standing first, then supine. This protocol was chosen to

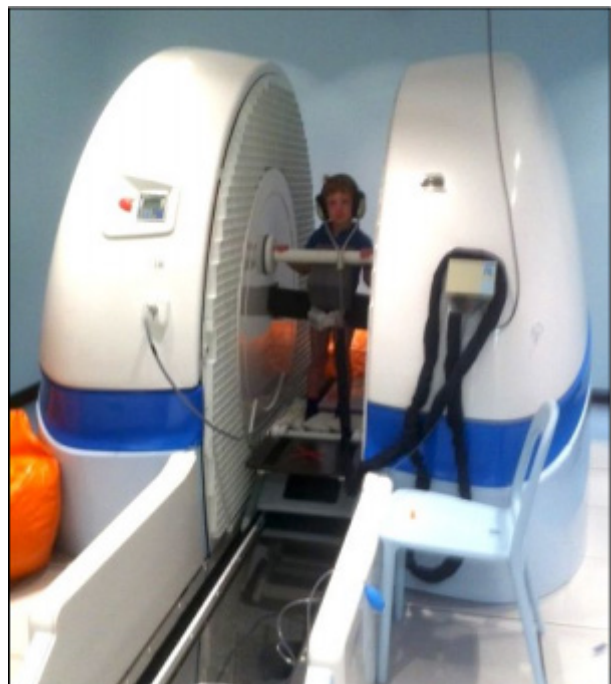


Fig. 1

Standing position for a child during the 2.5 minute weightbearing MRI scan. Foam blocks are used to hold the child in comfortable resting position.

limit the time in the scanner to what could reasonably be tolerated by a child with an irritable hip, while balancing adequate image quality.

Digital measurements

Digital measurements were performed using MicroDicom DICOM viewer (2017, Sofia, Bulgaria). Quantitative measurements on femoral head width, height and lateral extrusion were made, plus a qualitative assessment of femoral head shape. Femoral head width was measured as the widest point of the cartilaginous femoral head in the plane of the physis. Femoral head height was the highest point of the cartilaginous epiphysis in a plane perpendicular to the width. Lateral extrusion was measured as the maximal amount of cartilaginous femoral head lateral to Perkin's line. The lateral bony acetabulum and lateral cartilaginous edge of the femoral head were the clearest landmarks for making this measurement. Representative measurements can be seen in Figure 2. Overall shape was judged to be round, oval, or flattened. Supine to standing measurements were compared. Contralateral unaffected hips were used as controls. Sub-analysis by LCPD stage was performed.

Measurements were made using the agreed protocol by two independent reviewers and repeated at a one-month interval, giving four repeated results for each parameter measured. Intra and inter-observer reliability was calculated via intraclass *r* (ICC) using R (R Foundation for Statistical Computing, Vienna, Austria). Comparison

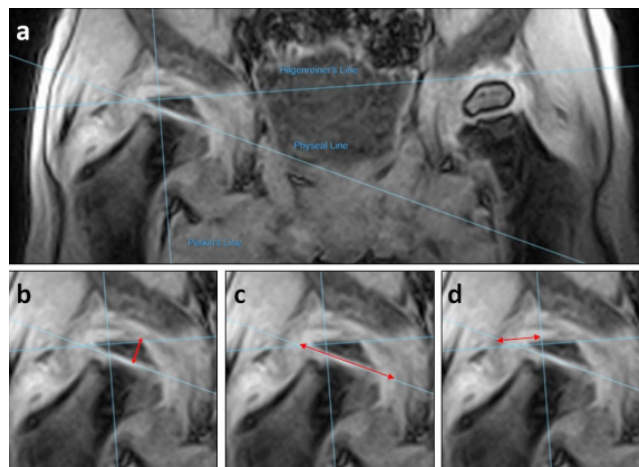


Fig. 2

Illustration of digital measurements made: a) standard reference lines; b) femoral head height; c) femoral head width; d) lateral extrusion.

of femoral head morphology from supine to standing was made of LCPD affected and contralateral unaffected femoral heads.

Results

Standing weightbearing and supine MRI scans were performed on ten children with LCPD. One child was excluded for inability to tolerate the scan protocol. Thus, nine children with LCPD (seven male, two female), with a mean age 5.3 years (4 to 8), had both standing and supine MR scans successfully completed using this newly developed protocol. Two of these patients had bilateral LCPD, thus eleven LCPD hips in nine children were included for analysis of femoral head morphology, alongside seven unaffected contralateral hips. Five hips were in early-stage (1 or 2) (all unilateral) and six hips demonstrated late-stage LCPD (3 or 4) (two unilateral, four bilateral hips) on plain radiograph (Table 1). None of these femoral heads had had any surgical intervention at the time of the MRI scan.

For both inter- and intrarater reliability of measurements, ICC values were graded good to excellent. Femoral head height and width measurements all demonstrated 'excellent' R values (inter-rater 0.86 and 0.84 respectively, intrarater 0.98 and 0.99 respectively). ICC measurements of extrusion were 'good' (R = 0.67 and 0.78 respectively).

Small changes were demonstrated in the seven contralateral unaffected hips on weightbearing. On the standing weightbearing MRI, a decrease in femoral head width (mean -0.06 ± 0.2 mm; 0.2% change), decrease in femoral head height (mean 0.01 ± 0.4 mm, 0.05% change), and increase in lateral extrusion (mean 0.01 ± 0.5 mm, 0.1% change) was detected compared to the supine scans. There was no qualitative change in femoral head shape of unaffected hips.

Table I. Demographic data of children in the study, alongside percentage change in femoral head morphology observed from supine to standing. Also included is the mean percentage change in femoral head shape of the seven contralateral unaffected hips.

Age	Sex	Side	Stage	Femoral head width	Femoral head height	Lateral extrusion
6	M	Right	1B	+ 14	- 11	+ 23
4	M	Right	2A	+ 6	- 11	+ 26
8	F	Right	2A	+ 1	- 17	+ 4
5	M	Left	2A	+ 10	- 10	+ 23
7	M	Right	2A	+ 6	- 13	- 9
6	M	Right	3A	- 1	+ 1	+ 14
4	M	Left	3A	- 3	- 31	+ 9
4	M	Left	3A	0	- 17	+ 10
4	M	Right	3A	+ 3	- 16	- 27
5	F	Left	3B	- 2	- 8	+ 4
5	F	Right	4	+ 1	- 11	- 2

More marked changes were demonstrated in hips in the early stages of LCPD on weightbearing. On standing weightbearing MRI, all early-stage hips demonstrated an increase in femoral head width (mean 2.5 mm (\pm 2.0 mm), mean 7.2% increase), and a decrease in femoral head height (mean 1.2 mm (\pm 0.2 mm), mean 12.4% decrease). All but one demonstrated an increase in lateral extrusion (median 2.5 mm (range -1.15 to 2.8 mm), median 23% increase) on standing weightbearing MRI compared to supine (Tables I and II). Qualitatively, a deformity could be observed subjectively on LCPD affected femoral heads, becoming flattened on weightbearing, which was more pronounced in those in fragmentation than re-ossification, (Figure 3). No shape alteration was observed in the normal contra-lateral hips.

Some changes were also evident in the LCPD hips in the late stages (3 and 4), but to a lesser extent. Femoral head width showed little change on weightbearing, with a mean 0.2 mm decrease (\pm 1.0 mm), mean 0.4% decrease. Femoral head height decreased in a similar way to early-stage LCPD hips, with a mean loss of height of 1.4 mm (\pm 1.4 mm), mean 13.8% decrease. Negligible overall change in lateral extrusion was observed (median + 0.7 mm, (range -3.2 to + 1.1 mm)), median 6.5% increase, though the range was wide.

Discussion

This study is the first reported use of a standing weightbearing MRI in LCPD. For the first time, a dynamic deformity has been identified in femoral heads when the child is loading the hip, with flattening and widening of the femoral head, plus worsened lateral extrusion. This was more pronounced in those children in early-stage LCPD than late-stage, though numbers are small for this sub-analysis. Negligible change was observed in contralateral unaffected femoral heads. Strict non weightbearing in a porcine model results in minimal femoral head deformity.²⁶ This weightbearing study provides biomechanical evidence

Table II. Comparison of percentage change of femoral head morphology of Legg-Calvé-Perthes disease hips in early-stage versus late-stage versus contra-ateral unaffected hips.

Demographics		% change on standing (mean or median)		
Stage of LCPD	Age range, years	Femoral head width	Femoral head height	Lateral extrusion
Unaffected hips	4 to 8	- 0.2	- 0.05	+ 0.1
Early-stage	4 to 8	+ 7.2	- 12.4	+ 23.0
Late-stage	4 to 6	- 0.4	- 13.8	+ 6.5

in humans, for the first time, to support this previous landmark paper. The success of this pilot study opens avenues to further explore the effect of loading of LCPD femoral heads, translated to humans rather than in vivo.

The findings presented here add weight to the hypotheses that mechanical forces from weightbearing result in the deformation seen in LCPD.^{2,24-26} This supports the treatment strategy of limiting weightbearing in children in the early phases of LCPD, to protect from such dynamic deformation observed in this study. However, this is a pilot study with a small cohort thus further work is warranted.

As the study is novel, effect size and power calculations were unable to be performed prior to recruitment. Furthermore, following data acquisition of the nine children, sample size calculations were unable to be determined given the large standard deviations present. The range of deformation is small and the confidence intervals are, in relation, wide. Thus there remains risk of Type 1 and Type 2 errors. Observed changes in lateral extrusion were the broadest across the patient cohort. Extrusion could be affected by hip position as well as femoral head shape. Despite best efforts, hip position is subject to change in moving from standing to supine scans and may limit the utility of this measurement compared to femoral head width and height. Due to a small sample size for this pilot study, percentage change of shape rather than p-values were used. As such, further patient recruitment and data collection is required, including with children in all stages of the disease process in order to perform meaningful statistical calculations.

The tolerated time limit of weightbearing the affected hips was seen to be 2.5 minutes for children as young as four years of age to produce adequate, interpretable images. The brevity of scan duration, however, precluded multiplanar data, given the nature of MRI acquisition. As such, the measurements were limited to coronal plane only. No information was possible on axial or sagittal plane deformities, which undoubtedly also contribute to the patho-physiology. Scans were also subject to motion artifact. To acquire longer scans in this age group would require sedation, thus would not be amenable to weightbearing and would introduce risks of anaesthesia. Imaging quality is further limited by the low Tesla

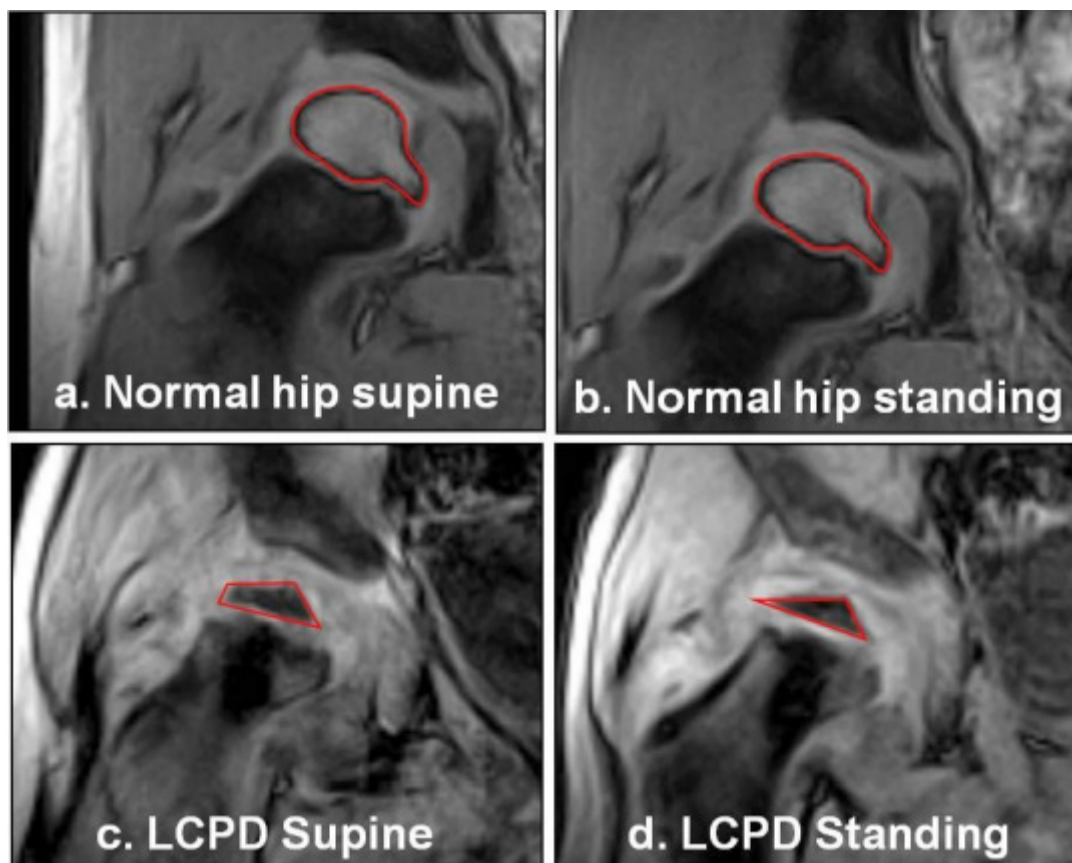


Fig. 3

Qualitative representation of femoral head deformity observed in those children with early-stage Legg-Calvé-Perthes disease (LCPD), compared to contralateral normal hips. The normal hips showed no visible deformation (3a & 3b). The resting deformity of the LCPD hips (3c) was exacerbated on weightbearing (3d). The cartilaginous outline is visible and the ossific nucleus, also deformed, is outlined in red.

magnet utilized. Despite the image quality, intra- and interobserver reliability was good to excellent.

A number of further measures could be taken to increase the accuracy of this study. Given the symptomatic and painful nature of the affected hips, altered and potentially partial weightbearing may have occurred during scans. Force plate analysis could be used to quantify the load taken on the affected hip. Despite lacking this additional data, changes in femoral head shape were consistently observed in the LCPD hips. It is unlikely that children did not weight bear on the unaffected hips, which demonstrated negligible deformity, supporting the notion that some weight at least was placed through the affected hip at the time of the scan. However, the deformation observed could not be quantified in relationship to force. Every measure was taken to reproduce the hip position and rotation when the child was maneuvered from standing to supine scan. However, measures could be taken to specify hip position, such as MRI-safe RSA. While reviewers were independent, they were not blinded to whether the scans were supine or standing, which is a potential bias. The study could be improved by using multiple observers,

not only for the measurements, but also classification of stage of disease, which has historically been fraught with variability.

This pilot study has demonstrated a successful and reproducible protocol for functional imaging of hips in children affected by LCPD under physiological loading. Adequate images were obtained to enable quantification and comparison of morphologic changes of LCPD femoral heads on weightbearing. These changes cannot, as yet, be linked to long-term changes as the ongoing visco-elasticity of these femoral heads is not known. However, these observed dynamic changes support a hypothesis of mechanically-induced deformation.

These novel MRI scans of affected LCPD hips under weightbearing conditions have provided direct evidence of a dynamic deformity that has not previously been observed. Such deformation was negligible in unaffected femoral head controls and was more marked in the early stages of the disease. This novel finding provides insight into the pathogenesis of femoral head deformity and has potential implications on treatment strategies, though further study is needed.

References

1. **Nguyen N-AT, Klein G, Dogbey G, McCourt JB, Mehlman CT.** Operative versus nonoperative treatments for Legg-Calvé-Perthes disease: a meta-analysis. *J Pediatr Orthop.* 2012;32(7):697–705.
2. **Berthume MA, Perry DC, Dobson CA, et al.** Skeletal immaturity, rostral sparing, and disparate hip morphologies as biomechanical causes for Legg-Calvé-Perthes' disease. *Clin Anat.* 2016;29(6):759–772.
3. **Froberg L, Christensen F, Pedersen NW, Overgaard S.** The need for total hip arthroplasty in Perthes disease: a long-term study. *Clin Orthop Relat Res.* 2011;469(4):1134–1140.
4. **Larson AN, Sucato DJ, Herring JA, et al.** A prospective multicenter study of Legg-Calvé-Perthes disease. *J Bone Joint Surg Am.* 2012;94(7):584–592.
5. **Stulberg SD, Cooperman DR, Wallensten R.** The natural history of Legg-Calvé-Perthes disease. *J Bone Joint Surg Am.* 1981;63(7):1095–1108.
6. **Hyman JE, Trupia EP, Wright ML, et al.** Interobserver and intraobserver reliability of the modified Waldenström classification system for staging of legg-calvé-perthes disease. *J Bone Joint Surg Am.* 2015;97(8):643–650.
7. **Joseph B, Varghese G, Mulpuri K, Narasimha Rao KL, Nair NS.** Natural evolution of Perthes disease: a study of 610 children under 12 years of age at disease onset. *J Pediatr Orthop.* 2003;23(5):590–600.
8. **Kim HT, Gu JK, Bae SH, Jang JH, Lee JS.** Does valgus femoral osteotomy improve femoral head roundness in severe Legg-Calvé-Perthes disease? *Clin Orthop Relat Res.* 2013;471(3):1021–1027.
9. **Herring JA, Kim HT, Browne R, disease L-C-P.** Legg-Calvé-Perthes disease. Part I: classification of radiographs with use of the modified lateral Pillar and Stulberg classifications. *J Bone Joint Surg Am.* 2004;86(10):2103–2120.
10. **Wiig O, Terjesen T, Svenningsen S.** Prognostic factors and outcome of treatment in Perthes' disease: a prospective study of 368 patients with five-year follow-up. *J Bone Joint Surg Br.* 2008;90(10):1364–1371.
11. **Herring JA, Kim HT, Browne R.** Legg-Calvé-Perthes disease. Part II: prospective multicenter study of the effect of treatment on outcome. *J Bone Joint Surg Am.* 2004;86-A(10):2121–2134.
12. **Kollitz KM, Gee AO.** Classifications in brief: the herring lateral Pillar classification for Legg-Calvé-Perthes disease. *Clin Orthop Relat Res.* 2013;471(7):2068–2072.
13. **Park MS, Chung CY, Lee KM, Kim TW, Sung KH.** Reliability and stability of three common classifications for Legg-Calvé-Perthes disease. *Clin Orthop Relat Res.* 2012;470(9):2376–2382.
14. **Saran N, Varghese R, Mulpuri K.** Do femoral or salter innominate osteotomies improve femoral head sphericity in Legg-Calvé-Perthes disease? A meta-analysis. *Clin Orthop Relat Res.* 2012;470(9):2383–2393.
15. **Dimeglio A, Canavese F.** Imaging in Legg-Calvé-Perthes disease. *Orthop Clin North Am.* 2011;42(3):297–302.
16. **Eggl H, Drekonja T, Kaiser B, Dorn U.** Ultrasonography in the diagnosis of transient synovitis of the hip and Legg-Calvé-Perthes disease. *J Pediatr Orthop B.* 1999;8(3):177–180.
17. **Kim HKW, Kaste S, Dempsey M, Wilkes D.** A comparison of non-contrast and contrast-enhanced MRI in the initial stage of Legg-Calvé-Perthes disease. *Pediatr Radiol.* 2013;43(9):1166–1173.
18. **Neal DC, O'Brien JC, Burgess J, Jo C, Kim HKW.** Quantitative assessment of synovitis in Legg-Calvé-Perthes disease using gadolinium-enhanced MRI. *Journal of Pediatric Orthopaedics B.* 2015;24(2):89–94.
19. **Sankar WN, Thomas S, Castañeda P, et al.** Feasibility and safety of perfusion MRI for Legg-Calvé-Perthes disease. *J Pediatr Orthop.* 2014;34(7):679–682.
20. **Kim HKW, Wiesman KD, Kulkarni V, et al.** Perfusion MRI in early stage of Legg-Calvé-Perthes disease to predict lateral Pillar involvement: a preliminary study. *J Bone Joint Surg Am.* 2014;96(14):1152–1160.
21. **Du J, Lu A, Dempsey M, Herring JA, Kim HKW.** Mr perfusion index as a quantitative method of evaluating epiphyseal perfusion in Legg-Calvé-Perthes disease and correlation with short-term radiographic outcome: a preliminary study. *J Pediatr Orthop.* 2013;33(7):707–713.
22. **Yoo WJ, Choi IH, Cho T-J, et al.** Risk factors for femoral head deformity in the early stage of Legg-Calvé-Perthes disease: Mr contrast enhancement and diffusion indexes. *Radiology.* 2016;279(2):562–570.
23. **Yoo WJ, Kim Y-J, Menezes NM, Cheon J-E, Jaramillo D.** Diffusion-Weighted MRI reveals epiphyseal and metaphyseal abnormalities in Legg-Calvé-Perthes disease: a pilot study. *Clin Orthop Relat Res.* 2011;469(10):2881–2888.
24. **Joseph B, Nair NS, Narasimha Rao KL, Mulpuri K, Varghese G.** Optimal timing for containment surgery for Perthes disease. *J Pediatr Orthop.* 2003;23(5):601–606.
25. **Nduaguba AM, Sankar WN.** Osteonecrosis in adolescent girls involved in high-impact activities: could repetitive Microtrauma be the cause?: a report of three cases. *JBJS Case Connect.* 2014;4(2):e35.
26. **Kim HK, Aruwajoye O, Stetler J, Stall A.** Effects of non-weight-bearing on the immature femoral head following ischemic osteonecrosis: an experimental investigation in immature pigs. *J Bone Joint Surg Am.* 2012;94(24):2228–2237.
27. **Buchan LL, Zhang H, Konan S, et al.** Open-MRI measures of CAM intrusion for hips in an anterior impingement position relate to acetabular contact force. *J Orthop Res.* 2016;34(2):205–216.
28. **Macri EM, d'Entremont AG, Crossley KM, et al.** Alignment differs between patellofemoral osteoarthritis cases and matched controls: an upright 3D MRI study. *J Orthop Res.* 2019;37(3):640–648.

Author information:

- A. Aarvold, BSc(Hons) MBChB MFST FRCSEd(T&O) DM, Consultant Paediatric Orthopaedic Surgeon & Honorary Associate Professor, Southampton Children's Hospital, Southampton, UK; Department of Orthopaedics, University of British Columbia, Vancouver, British Columbia, Canada.
- R. Lohre, MD
- H. Chhina, MSc
- K. Mulpuri, MBBS; MS (Ortho); MHSc (Epi); FRCSC, Associate Professor
- A. Cooper, FRCSC, Clinical Associate Professor
Department of Orthopaedics, University of British Columbia, Vancouver, British Columbia, Canada.

Author contributions:

- A. Aarvold: Designed the study, Carried out data collection and analysis, Prepared the manuscript.
- R. Lohre: Data analysis and manuscript preparation.
- H. Chhina: Designed the study, Carried out data collection and analysis, Prepared the manuscript.
- K. Mulpuri: Designed the study, Carried out analysis, Prepared the manuscript.
- A. Cooper: Designed the study, Carried out data collection and analysis, Prepared the manuscript.

Funding statement:

- The author or one or more of the authors have received or will receive benefits for personal or professional use from a commercial party related directly or indirectly to the subject of this article. In addition, benefits have been or will be directed to a research fund, foundation, educational institution, or other non-profit organization with which one or more of the authors are associated.

ICMJE COI statement:

- A. Cooper reports grants from BC Children's Hospital Research Institute, Rare Disease Foundation Microgrant, Pediatric Orthopaedic Society of North America Research Grant, and BC Children's Hospital Research Institute. The author also reports consultancy from Vilex and from Orthopediatrics, and grants/grants pending from Vilex and from BC Children's Hospital Foundation, which are unrelated to this article. K. Mulpuri reports grants/grants pending (research support) from Pega Medical (International Bone Health and Mobility Collaboration Projects), Allergan, Johnson & Johnson, IPSEN, Depuy Synthes, Medical Allied Staff Engagement Society, BC Children's Hospital Research Institute, I'm a HIPpy Foundation, Canadian Orthopaedic Foundation, Pediatric Orthopaedic Society of North America, and AO Foundation, all of which are unrelated to this article. The author further reports royalties from Pega Medical, and stock/stock options from Paradigm Creatives, which are also unrelated to this article.

Acknowledgements:

- We would like to thank Dr Dave Wilson from the Centre for Hip Health and Mobility for his contribution towards this pilot study.

Ethical review statement:

- Institutional ethics review was completed prior to data collection (CW15 0002/H14 03407)

©2020 Author(s) et al. This is an open-access article distributed under the terms of the Creative Commons Attribution licence (CC-BY-NC-ND), which permits unrestricted use, distribution, and reproduction in any medium, but not for commercial gain, provided the original author and source are credited. Standard